

Accepted Article

Title: Integrated Capture and Conversion of CO₂ to Methane using a Water-lean, Post-Combustion CO₂ Capture Solvent

Authors: David Heldebrant, Jotheeswari Kothandaraman, Johnny Saavedra Lopez, Yuan Jiang, Eric D. Walter, Sarah D. Burton, and Robert A. Dagle

This manuscript has been accepted after peer review and appears as an Accepted Article online prior to editing, proofing, and formal publication of the final Version of Record (VoR). This work is currently citable by using the Digital Object Identifier (DOI) given below. The VoR will be published online in Early View as soon as possible and may be different to this Accepted Article as a result of editing. Readers should obtain the VoR from the journal website shown below when it is published to ensure accuracy of information. The authors are responsible for the content of this Accepted Article.

To be cited as: *ChemSusChem* 10.1002/cssc.202101590

Link to VoR: <https://doi.org/10.1002/cssc.202101590>

FULL PAPER

Integrated Capture and Conversion of CO₂ to Methane using a Water-lean, Post-Combustion CO₂ Capture Solvent

Jotheeswari Kothandaraman, Johnny Saavedra Lopez, Yuan Jiang, Eric D. Walter, Sarah D. Burton, Robert A. Dagle, and David J. Heldebrant*

Abstract: Integrated Carbon Capture and Conversion of CO₂ into materials (IC³M) is an attractive solution to meet global energy demand, reduce our dependence on fossil fuels, and lower CO₂ emissions. Herein, using a water-lean post-combustion capture solvent, (N-(2-ethoxyethyl)-3-morpholinopropan-1-amine) (2-EEMPA), >90% conversion of captured CO₂ to hydrocarbons, mostly methane, is achieved in the presence of a heterogeneous Ru catalysts under relatively mild reaction conditions (170 °C and <15 bar H₂ pressure). The catalytic performance was better in 2-EEMPA than aqueous 5M monoethanol amine (MEA). Operando nuclear magnetic resonance (NMR) study showed in situ formation of N-formamide intermediate, which underwent further hydrogenation to form methane and other higher hydrocarbons. The technoeconomic analyses (TEA) showed that the proposed integrated process can potentially improve the thermal efficiency by 5% and reduce the total capital investment and minimum synthetic natural gas (SNG) selling price by 32% and 12% respectively compared to conventional Sabatier process, highlighting the energetic and economic benefits of integrated capture and conversion. Methane derived from CO₂ and renewable H₂ sources is an attractive fuel, and it has great potential as a renewable hydrogen carrier as an environmentally responsible carbon capture and utilization approach.

Introduction

Carbon capture, utilization, and storage (CCUS) has been widely considered as a solution to reduce the CO₂ emitted into the atmosphere, thus mitigating global warming, ocean acidification, and climate change.^[1] Amine-based solvents are commonly employed as solvents to capture CO₂, which then is released, compressed, and transported/stored to reduce CO₂ emissions from large scale industrial processes.^[2] Significant investments are being made in carbon capture technologies, but the cost associated with separation, compression, transportation, and storage is still economically prohibitive. On the other hand, CO₂ is an attractive and inexpensive C₁ feedstock to produce value-added chemicals and fuels such as methane, methanol, ethanol, dimethylcarbonate, formic acid, CO, cyclic carbonates, methylformate, polycarbamates, and polycarbonates.^[3, 4]

The direct conversion of captured CO₂ overcomes the challenges associated with the CCUS as the exothermic hydrogenation offsets the energy required for the regeneration of carbon capture solvent. There has been a surge in the literature for integrated capture and conversion of CO₂.^[3] While advances have been made in reducing CO₂ to chemicals and fuels, the majority of amine and alcohol-based capture solvents (used by us and others) for thermocatalytic conversion are not viable solvents for CO₂ capture as they are costly, too viscous (eg. polyethylenimine), or volatile (e.g., triethylamine/ethanol) to be used in post-combustion CO₂ capture. With the groundwork reactivity demonstrated, there is a need to apply this knowledge and design reactions and conditions that could proceed in promising carbon capture solvents.

Aqueous systems have a higher energy demand and cost compared to water-lean solvents.^[5] The commercially used aqueous post-combustion solvents (e.g., 5M MEA) are not suitable for combined capture and thermocatalytic hydrogenation to products that involve the formation of water as a by-product since the water shifts the equilibria backward (e.g., methanol, ethanol, methane, and others). Thus, the water-lean solvents are viable for thermocatalytic reductions because of the limited amount of water. Another advantage of water-lean capture solvents is the higher physical solubility of CO₂ that can be dissolved as compared to aqueous solvents, lowering the pressures of CO₂ required to promote the reaction. We note that there are elegant electrocatalytic approaches for utilizing CO₂ in aqueous carbon capture solvents such as 5M aqueous MEA, though such approaches decompose CO₂ into CO and proceed to make products via conventional synthesis gas.^[6] Nonetheless, demonstrable examples of thermocatalytic reduction of CO₂ in real solvents are limited.

Here, we show the combined capture and thermocatalytic conversion of CO₂ to methane using an advanced water-lean post-combustion capture solvent with the lowest total costs of capture (\$47.1/tonne CO₂) of most of the reported CO₂ capture technologies.^[5b] The required H₂ for this process can be obtained from renewable energy sources, namely, wind, solar, geothermal, or biomass. Synthetic natural gas (SNG) is a type of gas that serves as a substitute for natural gas and is suitable for transmission in natural gas pipelines, consisting primarily of methane, and small amounts of light hydrocarbons, nitrogen, etc.^[7] It is considered as a promising sustainable energy storage material to efficiently integrate intermittent renewable energy sources into the electrical grid. Furthermore, SNG is also attractive because the existing natural gas infrastructure can be readily adapted.

Materials with dual function have been reported in the literature for combined CO₂ capture and conversion to methane.^[8] These materials are composed of a sorbent and catalytic active component. The oxides (e.g., CaO) and carbonates (e.g.,

Dr. Jotheeswari Kothandaraman, Dr. Johnny Saavedra Lopez, Dr. Yuan Jiang, Dr. Eric D. Walter, Dr. Sarah D. Burton, Mr. Robert A. Dagle and Dr. David J. Heldebrant*
Pacific Northwest National Laboratory, Advances Energy Systems,
902 Battelle Blvd, Richland, Washington 99352, USA
E-mail: jotheeswari.kothandaraman@pnnl.gov,
johnny.saavedralopez@pnnl.gov, yuan.jiang@pnnl.gov,
Eric.Walter@pnnl.gov, Sarah.Burton@pnnl.gov,
Robert.Dagle@pnnl.gov, david.heldebrant@pnnl.gov

Supporting information for this article is given via a link at the end of the document.

FULL PAPER

Na_2CO_3) are used as CO_2 sorbent. Metals such as Ni, Ru, and Rh act as catalysts for the conversion of adsorbed CO_2 . However, both the adsorption and hydrogenation reaction are performed at high temperature (300 °C–750 °C). Other proposed technologies include utilizing traditional aqueous amine CO_2 capture solvents and employing gas-phase CO_2 hydrogenation using methane synthesis catalysts. However, these approaches are

economically less viable due to the energy penalty of CO_2 separation and compression prior to the gas-phase CO_2 hydrogenation.

Results and Discussion

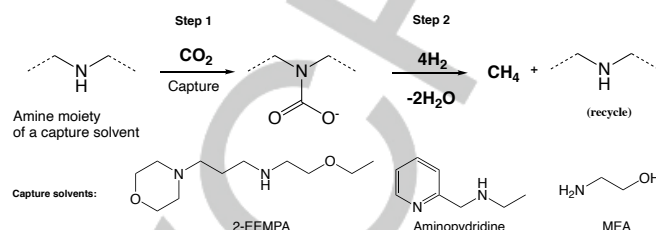
2-EEMPA, was chosen for the initial batch reactor studies to form methane from CO_2 (Table 1). 2-EEMPA is a single-component, water-lean post-combustion CO_2 capture solvent with high durability, low total capture cost and high capture efficiency (>95% with coal derived flue gas).^[5a] A post-combustion capture solvent is preferred as it can separate CO_2 from dilute streams. When CO_2 is captured in 2-EEMPA, it forms a carbamate intermediate, which is an excellent intermediate to accomplish CO_2 hydrogenation instead of using gaseous CO_2 at high-pressure. Gas-phase CO_2 methanation has been shown to be catalyzed by transition metals such as Ru, Rh, Ni, Co, Pt, and Pd.^[9] Among these metals, Ru is often reported as a most active catalyst for CO_2 methanation. Thus, we decided to screen a commercial Ru catalyst, Ru/ Al_2O_3 , for hydrogenation of EEMPA-carbamate.

There was no detectable amount of methanol observed in the presence of Ru/ Al_2O_3 (Table 1, entry 1). However, >75% conversion of captured CO_2 was observed with 87% selectivity for methane at 170 °C. Small amounts of ethane and other higher hydrocarbons were also detected by gas chromatography (GC). CO_2 methanation was also observed at low temperatures (145 °C and 120 °C (temperatures where CO_2 is thermally released from 2-EEMPA), entry 2 and 3, Table 1), albeit at slower rate. It is noteworthy that in the presence of a capture solvent (entry 1, Table 1), ethane and higher hydrocarbons are formed at higher selectivity than gas-phase CO_2 methanation (entry 4, Table 1).

Only small amounts of methane were formed in presence of Pd and Cu catalysts (Table 5–7, Table 1). The gas-phase methanation of CO_2 over Ni catalysts has been shown in the literature.^[10] However, the Ni/ Al_2O_3 was not very active in the presence of 2-EEMPA solvent (entry 8, Table 1). The Ru on alumina support performed better than the carbon support (entry 1 vs entry 9, Table 1). The use of aminopyridine-based CO_2 capture solvent decreased the methane yield (entry 10, Table 1). The commonly used aqueous capture solvent, MEA, was also screened (entry 11, Table 1). In 30wt% aqueous MEA solution, <20% conversion of CO_2 to hydrocarbon was observed. The CO_2

conversion is slower in the aqueous solvent because the excess water in the reaction does not favor the dehydration step. This shows water-lean solvents are a superior option for integrated capture and conversion. A prolonged reaction time in EEMPA solvent resulted in >90% conversion of captured CO_2 (entry 12, Table 1).

Table 1. Hydrogenation of captured CO_2 to methane



Entry	Catalyst	T (°C)	t (h)	CO ₂ conversion (%)	Selectivity (%)		
					CH ₄	C ₂ H ₆	C ₃ -C ₄
1	5wt% Ru/ Al_2O_3	170	3	75.8	87.4	4.6	8
2	5wt% Ru/ Al_2O_3	145	3	20.4	94	2.2	3.7
3	5wt% Ru/ Al_2O_3	120	3	3.6	98	2	0
4 ^[a]	5wt% Ru/ Al_2O_3	170	3	82.6	99	0.8	0.2
5	5wt% Pd/ $\text{ZnO}/\text{Al}_2\text{O}_3$	170	3	<1	trace	-	-
6	5wt% Pd/ ZnO	170	3	0	-	-	-
7	64wt% Cu/ $\text{ZnO}/\text{Al}_2\text{O}_3$	170	3	<1	trace	-	-
8	35wt% Ni/alumina	170	3	1.3	97.1	2.9	-
9	5wt% Ru/C	170	3	12.3	90.2	5.9	3.8
10 ^[b]	5wt% Ru/ Al_2O_3	170	3	21.6	91.8	8	0.2
11 ^[c]	5wt% Ru/ Al_2O_3	170	3	29.8	79.2	5.2	15.6
12	5wt% Ru/ Al_2O_3	170	6	>99	87.1	3.8	9
13 ^[d]	5wt% Ru/ Al_2O_3	170	6	73.6	92.2	6.8	1

Initial $P(\text{H}_2)$ = 15 bar, t = 3 h, captured CO_2 = ~14.5 mmol, 2-EEMPA = 5 g (23 mmol), catalysts = 200 mg, T = 170 °C, the capture solvent was sparged with CO_2 for a given time (~15 min - 1 h depending on the capture solvent) to load ~15 mmol of CO_2 , the amount of CO_2 captured was determined gravimetrically with an analytical balance.^[a] using CO_2 gas and in the absence of EEMPA, ^[b]aminopyridine (5g) – 15.2 mmol CO_2 captured, ^[c]30wt% MEA in water – 15.4 mmol CO_2 captured, ^[d]4wt% water in 2-EEMPA-carbamate was used. CO_2 conversion = $(\text{mol CH}_4 * 1 + \text{mol C}_2\text{H}_4 * 2 + \text{mol C}_3\text{-C}_4 * 3.5) / (\text{mol CO}_2 * 1)^{-1}$

The hydrogenation of EEMPA-carbamate was performed with H_2O and/or O_2 in order to understand the influence of impurities on catalytic conversion. Water loading was set at ~4wt% H_2O , its projected steady state water load in operation. The presence of water lowered the reaction rate, and the CO_2 conversion decreased to 74% (entry 13, Table 1) from 99% (entry 10, Table 1). Note that the O_2 solubility is in ppm quantities for most amine-based carbon capture solvents,^[11] thus most of the O_2 from flue gas is expected to leave from absorber, and only trace amounts will be carried from CO_2 -rich solvent and fed into the methanation reactor. A reaction performed in the presence of O_2 (with a O_2/Ru ratio of 10) under similar conditions (Table 1, entry 13) showed no change in the selectivity and conversion.

FULL PAPER

We extended the favorable conditions identified for a batch process to a continuous flow process. We calculated a Weight Hourly Space Velocity (WHSV) equivalent for a continuous reaction system (fixed bed) using reaction time, solvent, and catalyst loading in the batch system. In the presence of the Ru/Al₂O₃ catalyst, we performed CO₂ methanation at 170 °C with 10 wt% CO₂ loaded 2-EEMPA. Figure 1 and Table 2 show increase in CO₂ conversion at lower WHSV (higher contact time) while selectivity toward methane remained unaffected, making it the primary product (>86% selectivity); other secondary products formed include ethane, methanol, and ethanol. Methanol (and ethanol) selectivity drastically decreased at higher contact time from 7% (WHSV=0.3 h⁻¹) to <1% (WHSV=0.03 h⁻¹), indicating that these alcohols are reactive species and that upon formation they are quickly reduced to methane and ethane. Increase in the reaction temperature from 170 °C to 190 °C with a WHSV (g_{CO2} g_{cat}⁻¹ h⁻¹) of 0.3 h⁻¹, increased the CO₂ conversion from 17.6 to 52.1%, while methane selectivity remained the same (entry 1 vs 3, Table 2). Overall, prolonged contact time and higher temperature, decreased the selectivity to alcohols and increased the selectivity to methane and ethane (Table 2).

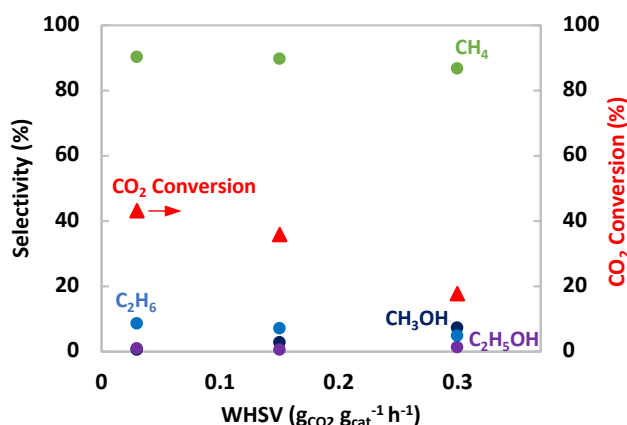


Figure 1. Selectivity (left axis) and CO₂ conversion (right axis) vs Weight Hourly Space Velocity (WHSV) in fixed bed experiments using 2-EEMPA solvent (10 wt% CO₂ load) over 5 wt% Ru/Al₂O₃ catalyst at 170 °C. Reaction conditions: 1g catalyst load, 60 bar, 38 sccm H₂, 5 sccm N₂. Change in WHSV is achieved by changing the liquid feed flow (0.05, 0.025, 0.005 mL min⁻¹). CO₂ conversion = ((mol CH₄*1 + mol C₂H₄*2 + mol CH₃OH*1 + mol C₂H₅OH*2)*min⁻¹) (mol CO₂ min⁻¹)⁻¹

Table 2. Conversion and selectivity in fixed bed experiments using 2-EEMPA solvent (10 wt% CO₂ load) over 5 wt% Ru/Al₂O₃ catalyst.

Entry	WHSV (g _{CO2} g _{cat} ⁻¹ h ⁻¹)	CO ₂ conversion (%)	Selectivity (%)			
			CH ₄	C ₂ H ₄	CH ₃ OH	C ₂ H ₅ OH
1	0.3	17.6	86.7	4.8	7.2	1.2
2	0.03	43.2	90.1	8.5	0.4	0.9
3 ^[a]	0.3	52.1	87.7	9.1	2.7	0.6

Reaction conditions: 1g catalyst load, 170 °C, 60 bar, 38 sccm H₂, 5 sccm N₂. Change in WHSV is achieved by changing the liquid feed flow (0.05, 0.025, 0.005 mL min⁻¹). ^[a]190 °C, CO₂ conversion = ((mol CH₄*1 + mol C₂H₄*2 + mol CH₃OH*1 + mol C₂H₅OH*2)*min⁻¹) (mol CO₂ min⁻¹)⁻¹

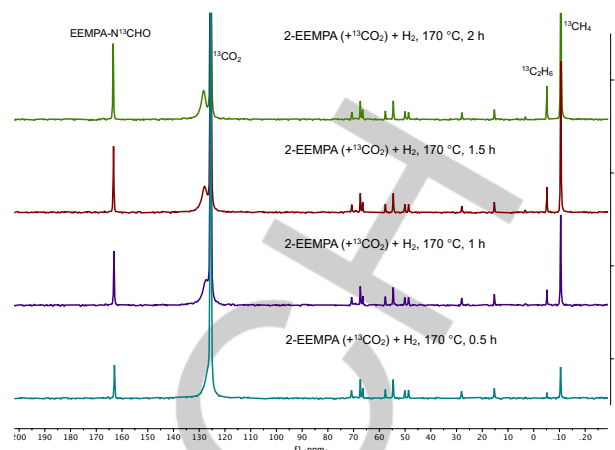
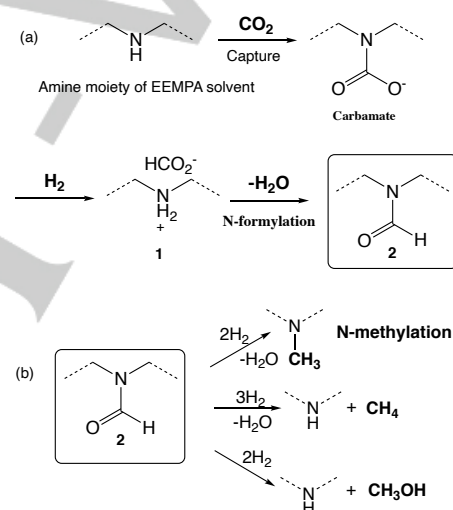


Figure 2. Methanation of 2-EEMPA-carbamate in the presence of 5wt% Ru/Al₂O₃ catalyst at 170 °C under 70 bar H₂ (initial pressure).



Scheme 1. Hydrogenation of CO₂ to different products via formamide intermediate.

Operando magic angle spinning (MAS) ¹³C NMR spectroscopy was performed to identify the reactive species and understand the reaction mechanism. NMR analysis of hydrogenation of CO₂ captured EEMPA solution in the presence of Ru/Al₂O₃ showed in situ formation of EEMPA N-CHO (**2**) and simultaneous formation of methane and ethane (Figure 2). It is notable that alcohols were observed in the continuous flow experiments at short contact time or at low temperatures but not in the batch or in situ NMR experiments, suggesting alcohols are short-lived reactive species that quickly undergo hydrogenation to form hydrocarbons. Based on this observation, the methanation in 2-EEMPA is proposed to proceed as shown in Scheme 1a. The EEMPA N-CHO (**2**) is formed via formate intermediate (**1**), which, depending on the catalyst and reaction conditions (Scheme 1b), then forms many products, namely, methanol, methane, and N-methylated capture solvent. N-methylation of capture solvent will lead to solvent deactivation as the active amine moiety (-NH) is not available to form carbamate species and thus preventing the successive reuse of the capture solvent for continuous CO₂

FULL PAPER

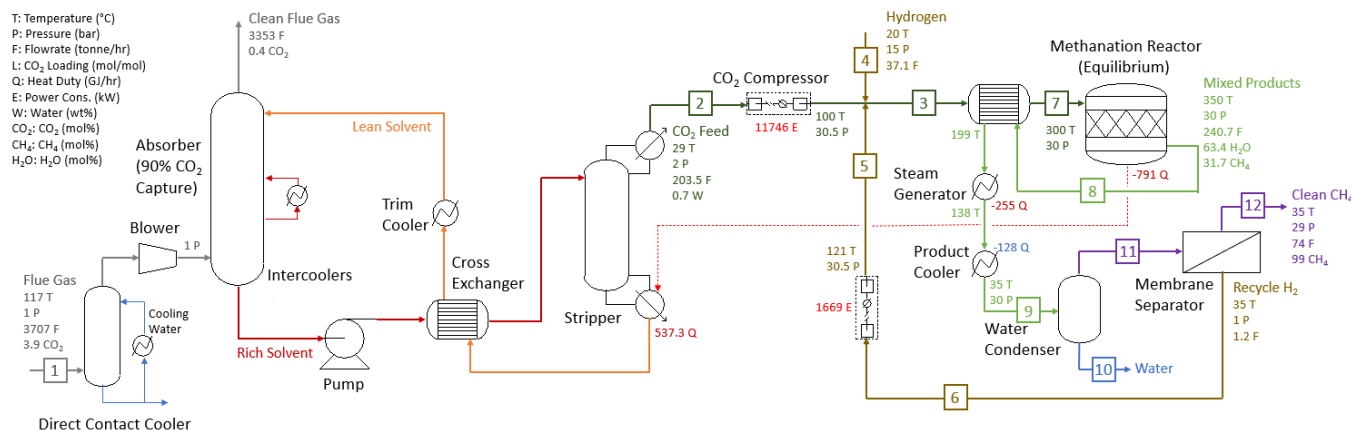


Figure 3. Literature FG-to-SNG process.^[13, 16, 17]

capture and utilization. It is important to note that no N-methylation of 2-EEMPA was observed in any of the experiments

The gas-phase CO₂ methanation typically occurs via CO as an intermediate species. In the solvent promoted methanation process demonstrated here, there was no detectable amount of CO in both GC and NMR analysis as the reaction temperature is low for the reverse water gas shift (RWGS) reaction. However, hydrogenation of metal bound CO (in situ formed from CO₂) to methane can also take place without forming gaseous CO.^[12] To test the involvement of EEMPA N-CHO, **2** in the reaction mechanism, we hydrogenated a surrogate N-formyl species, N-formylpiperidine, at 170 °C under 30 bar H₂. Without addition of external CO₂, >80% conversion to methane in the gas phase was observed after the reaction, which shows that both CO and N-formamide routes are possible in the solvent promoted CO₂ methanation reaction. To the best of our knowledge, this is the first demonstration of integrated low-temperature thermocatalytic capture and conversion of CO₂ to methane in an economically viable post-combustion CO₂ capture solvent.

The TEA was conducted for the proposed and the literature processes that produce SNG from flue gas (FG) from natural gas combined cycle (NGCC) power plants. It is assumed the CO₂ capture and conversion plant is co-located with the NGCC power plant. Therefore, the scale of the plant was set to be the same as the NETL's NGCC baseline with a net power output of 550MW. In the literature process (as shown in Figure 3) model, FG is first sent to a carbon capture process that uses Cansolv technology.^[13] Here, CO₂ in the FG is captured in the absorber and released in the stripper at about 2 bars with thermal regeneration. The pure CO₂ from the stripper is compressed and mixed with hydrogen before going to the methanation reactor, where the Sabatier reaction ($\text{CO}_2 + 4\text{H}_2 \rightarrow \text{CH}_4 + 2\text{H}_2\text{O}$; $\Delta H = -165\text{kJ/mol}$) takes place at 350 °C and 30 bar with the Ru/Al₂O₃ catalyst. The Sabatier reaction is exothermic, and most of the reaction heat is used to supply the energy required in the CO₂ stripper, while the remaining is used for power generation. The hot product from the methanation reactor is used to preheat reactor feed. By-product water is removed by condensation. The unconverted hydrogen is recovered in a membrane separator and recycled back to the reactor.

The proposed solvent promoted methanation process uses the IC³M technology enabled by the water-lean solvents developed by PNNL (2-EEMPA in this case). As shown in Figure 4, instead of stripping off CO₂ from the rich solvent and compressing vapor-phase CO₂, in the IC³M process, the entire

rich solvent from the absorber (containing condensed-phase CO₂) is pumped to 15 bar and the mixed with hydrogen for Ru/Al₂O₃ catalyzed methanation. The product stream from the condensed-phase reactor contains SNG, solvent, and by-product water, which is cooled to 35 °C for downstream separation. As mentioned before, the methanation reaction is highly exothermic, and therefore, a significant amount of steam is generated for power generation. SNG is recovered in a flash drum by vapor–liquid separation. By-product water is removed by the pressure driven membrane process to prevent water accumulation in the system.^[14]

Table 3. Comparison between the proposed IC³M and literature^[13,16,17] FG-to-NG processes.

Process	Proposed	Literature
Scale (Million MMBtu SNG/year)	33.8	33.8
Carbon Capture Condition		
Lean / Rich Loading (mol CO ₂ /mol solvent)	0 / 0.136	
Regeneration Heat Duty (GJ/tonne CO ₂)	≈ 2.5	2.65 ^[13]
CO ₂ Capture Cost (\$/tonne CO ₂)		71 ^[13]
Methanation Condition		
Temperature (°C)	170	350 ^[16,17]
Pressure (bar)	15	30 ^[16,17]
CO ₂ Conversion (%)	99.8	99 ^[16,17]
Heat of Reaction (GJ/tonne CO ₂)	-3.75	-3.75
Key Performance Measures		
Thermal Efficiency (% HHV)	79.75	76.14
Hydrogen Consumption (kg/kg SNG)	0.503	0.505
CO ₂ Compression/Pump (kWh/tonne CO ₂)	18.33	57.95
Key Economic Measures		
Total Plant Cost (MM\$)	556.2	823.0
Minimum SNG Selling Price (\$/MMBtu)	25.0	28.4
Cost Distribution		
H ₂ Cost (\$/MMBtu SNG)	20.2	20.2
Carbon Credit (\$/MMBtu SNG)	-1.8	-1.8
O & M and Other Cost (\$/MMBtu SNG)	4.1	6.3
Capital Cost (\$/MMBtu SNG)	2.5	3.7

FULL PAPER

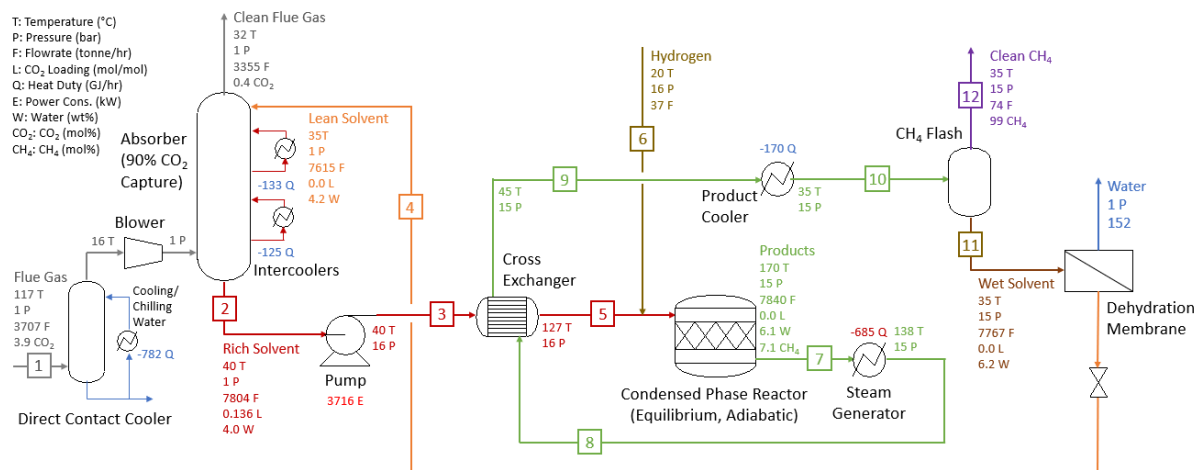


Figure 4. Proposed FG-to-SNG process with the IC³M technology.

As 2-EEMPA has a molecular weight of 216 g/mol, significantly higher than that of water, a nano filtration process^[15] with a pressure difference of 5–40 bar can be applied to partially remove water at 35 °C. The membrane process is not expected to take extra energy as the wet solvent from the reactor is already at an elevated pressure. Note that the proposed process aims to produce SNG instead of pure methane. Due to the relatively small size of the SNG process, instead of considering a stand-alone separation unit, SNG can be further processed in a typical natural gas processing plant along with conversional natural gas.^[7] Therefore, downstream separation is out of the scope of this work.

The NGCC power plant described in Case B31B in the National Energy Technology Laboratory (NETL) Rev3 Report, 2015^[13] was used as the baseline for plant scale (550 MW net power output) and FG condition (3.9 mol% CO₂, 8.4 mol% H₂O, 74.4 mol% N₂, 12.4 mol% O₂, and 0.9 mol% Argon). Process models were developed in Aspen Plus V10 to calculate mass and energy balance and to estimate equipment sizes for the entire IC³M process proposed by the researchers and the CO₂ conversion section of the literature FG-to-SNG process. For the literature FG-to-SNG process, the mass and energy balance as well as capital cost of the carbon capture section can be found in the NETL Report.^[13] The methanation process is modeled based on open literature.^[16,17] ENRTL-RK property package was used for the operations involving solvents, while Peng-Robinson equation-of-state was used for the operations not involving solvents. For EEMPA, property characteristics, performance testing of carbon capture and development of property models can be found in our previous publications.^[5] The condensed-phase methanation reactor is modeled as an adiabatic reactor in Aspen Plus with CO₂ conversion at equilibrium (similar to entry 12, Table 1). Entry 13 indicates a slight drop in CO₂ conversion by adding water and keeping the same reaction time. To understand whether this decrease is caused by chemical equilibrium or kinetics, chemical equilibrium calculations with and without H₂O in the feedstock was conducted in Aspen Plus using RGibbs reactor minimizing Gibbs free energy. The result indicates a less than 1% reduction in equilibrium CO₂ conversion by adding 4 wt% water to the feedstock at 170 °C. Therefore, a higher conversion is expected as reaction time increases. More details of modeling assumptions and equipment design can be found in

supplementary information. Aspen Process Economic Analyzer was used for capital cost estimation. The simple annualized cost approach described in PEP Yearbook^[18] was used to estimate the minimum SNG selling price with 15% rate of return (ROI) respectively in 2014 US dollars. In this TEA, the H₂ price and carbon credits were set to \$2.1/kg H₂ and \$35/tonne CO₂, in the base case. Figures 3 and 4 also present the operating condition and utility consumptions of major equipment as well as key stream information, including temperature, pressure, and concentration of key components. More details can be found in the supplementary information. Table 3 gives a detailed comparison between the proposed and literature FG-to-SNG processes, while Figure 5 presents a sensitivity study regarding H₂ price.

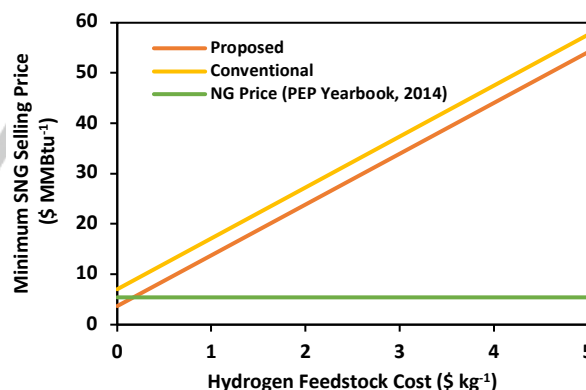


Figure 5. Impact of H₂ cost on the Minimum SNG Selling Price.

The results indicate that the proposed technology can potentially increase the thermal efficiency of the entire process by 5%, potentially reducing the energy consumption for CO₂ pressurization, total capital investment, O&M cost, and minimum SNG selling price of FG-to-SNG processing by 68%, 32%, 35%, and 12%, respectively. The reduction on the minimum SNG selling price is not as significant as the other performance and economic measures because the H₂ cost dominates the minimum SNG selling price (more than 70%), while H₂ consumptions of both processes are the same. The contribution from H₂ cost of this work agrees with open literature.^[16] Figure 5 suggests that the benefits of the proposed IC³M process over literature process increase as the H₂ price decreases.

FULL PAPER

Conclusions

In conclusion, we have demonstrated an efficient and cost-effective integrated carbon capture and utilization approach to produce SNG. Selective formation of hydrocarbons, primarily methane, was achieved from captured CO₂ at low temperatures and pressures using an advanced water-lean post-combustion capture solvent. Operando NMR showed formation of methane through a distinctive formamide reaction intermediate. The proposed IC³M approach offsets energy of capture with the energy of conversion, where the exothermicity of the hydrogenation is used to offset the endothermic regeneration of the capture solvent. The conversion of CO₂ captured in solution bypasses the energies associated with CO₂ compression and transportation that are inherently sunk in a conventional Sabatier process. Integration of these two units of operation could improve the thermal efficiency by 5% and reduce the total capital investment and minimize SNG selling price by 32% and 12% respectively compared to a conventional Sabatier process. We posit that other integrated approaches would exhibit similar energy and cost reductions, thereby creating attractive CO₂ utilization approaches, which could be deployed as a part of an all-of-the-above CCUS strategy.

Experimental Section

Materials: 5wt% Ru/Al₂O₃ and 5wt% Ru/C were obtained from Strem chemicals. 64wt% Cu/Zn/Al₂O₃ was purchased from Alfa Aesar. 2-EEMPA was synthesized by following the procedure reported in the literature^[5a, 19]. N-(2-Pyridinylmethyl)ethanamine was obtained from Sigma-Aldrich. 35wt% Ni/Al₂O₃ was synthesized by incipient wetness impregnation with nickel nitrate solution, followed by calcination in open air at 350 °C for 3 h. All other materials were purchased from commercial suppliers and used without further purification unless otherwise mentioned. MEA was purchased from Sigma-Aldrich. All deuterated solvents were purchased from Cambridge Isotope Laboratories, Inc. 1,3,5-Trimethoxybenzene (TMB) was added as an internal standard for NMR.

Standard procedure for batch experiments: A Parr reactor (100 mL) was charged with catalyst and CO₂ loaded capture solvent and sealed in a N₂-atmosphere glovebox. The reactor was then pressurized with H₂ (15 bar) and heated to 170 °C. The reactor was cooled to room temperature and the gas in the reactor head space was analyzed using a 2 channel Fusion MicroGC (Inficon). The remaining excess gas was released slowly after cooling the reactor to -78 °C. TMB was dissolved in acetonitrile and added as an internal standard to the reaction mixture and a small aliquot of the sample was analyzed by ¹H and ¹³C NMR experiments in CD₃CN.

Procedure for in situ high-pressure and high-temperature MAS-NMR: The MAS-NMR experiments were performed on an Agilent-Varian VNMRs NMR spectrometer equipped with a 7.05 T magnet, operating at 75.43 MHz for the ¹³C channel and 299.969 MHz for ¹H channel, and using a 5 mm Chemmagnetics design HXY probe. The rotors were Varian/Agilent style cavern rotors (Revolution NMR LLC), modified for high-pressure samples as described previously.^[20] 2-EEMPA (0.16 mmol) and 5wt% Ru/Al₂O₃ (8 mg) were transferred to a MAS-NMR rotor in a N₂-atmosphere glovebox. The rotor was charged with a ¹³CO₂ (0.28 mmol) and H₂ (0.8 mmol) at room temperature and heated to 170 °C. When the set temperature reached, the rotor was kept at this temperature while an array of ¹³C NMR spectra collected. A 45-degree pulse was used. A recycle delay of 30 seconds and spinning speed of 5 kHz were applied. The spectra were acquired with 64 scans, and acquisition time of 300 ms.

Standard procedure for continuous flow experiments: Fixed bed experiments were performed in a stainless-steel tubular reactor (3/8 nominal OD, 0.305 ID), the reactor wall is heated with a stainless-steel block (3 in) wrapped with a fiberglass heating tape (briskheat). Liquid is fed to the reactor using a high-pressure ISCO pump (Teledyne) and gases (H₂, N₂) are fed using mass flow controllers (Brooks). In a typical experiment, 1 g of catalyst (60-100 mesh) is loaded between quartz wool in the heated part of the reactor. Reaction conditions: pressure (60 bar) is controlled using a Tescom back pressure regulator, temperature (120 – 190 °C) is controlled using a digisense R/S controller. After reaction, liquid products are condensed and collected in a stainless-steel 50 mL cylinder maintained at 0 °C using recirculatory thermostat (VWR). Gas products are analyzed using a 4 channel Fusion MicroGC (Inficon), and liquid products are analyzed using liquid chromatography.

Acknowledgements

The authors would like to acknowledge the U.S. Department of Energy's (DOE's) Technology Commercialization Fund (TCF) and SoCalGas for co-funding this work. This material is based upon work supported by the DOE's Office of Science, Office of Basic Energy Sciences, Chemical Sciences, Geosciences, and Biosciences Division. The authors thank Dr. Phillip Koech and Dr. Deepika Malhotra for providing 2-EEMPA. The HT/HP solid-state NMR experiments were performed under proposal number 51704 at the Environmental Molecular Sciences Laboratory (EMSL), a Department of Energy (DOE) Office of Science user facility sponsored by the Office of Biological and Environmental Research. The Pacific Northwest National Laboratory is operated by Battelle for the DOE.

Keywords: CO₂ • CO₂ methanation • CO₂ Capture • CO₂ utilization • water-lean solvent • TEA

References

- [1] a) A. Al-Mamoori, A. Krishnamurthy, A. A. Rownaghi, F. Rezaei, *Energy Technol.* **2017**, *5*, 834-849; b) P. Gabrielli, M. Gazzani, M. Mazzotti, *Ind. Eng. Chem. Res.* **2020**, *59*, 7033-7045; c) J. Leclaire, D. J. Heldebrant, *Green Chem.* **2018**, *20*, 5058-5081; d) E. C. Ra, K. Y. Kim, E. H. Kim, H. Lee, K. An, J. S. Lee, *ACS Catal.* **2020**, *10*, 11318-11345; e) M. Bui, C. S. Adjiman, A. Bardow, E. J. Anthony, A. Boston, S. Brown, P. S. Fennell, S. Fuss, A. Galindo, L. A. Hackett, J. P. Hallett, H. J. Herzog, G. Jackson, J. Kemper, S. Krevor, G. C. Maitland, M. Matuszewski, I. S. Metcalfe, C. Petit, G. Puxty, J. Reimer, D. M. Reiner, E. S. Rubin, S. A. Scott, N. Shah, B. Smit, J. P. M. Trusler, P. Webley, J. Wilcox, N. Mac Dowell, *Energy Environ. Sci.* **2018**, *11*, 1062-1176; f) C. Hepburn, E. Adlen, J. Beddington, E. A. Carter, S. Fuss, N. Mac Dowell, J. C. Minx, P. Smith, C. K. Williams, *Nature* **2019**, *575*, 87-97.
- [2] a) P. Luis, *Desalination* **2016**, *380*, 93-99; b) D. Aaron, C. Tsouris, *Sep. Sci. Technol.* **2005**, *40*, 321-348; c) D. J. Heldebrant, P. K. Koech, V. Glezakou, R. Rousseau, D. Malhotra, D. C. Cantu, *Chem. Rev.* **2017**, *117*, 9594-9624; d) D. J. Heldebrant, J. Kothandaraman, in *Carbon capture and storage*, (Eds.: Mai Bui, N. M. Dowell), The Royal Society of Chemistry, **2020**, pp. 36-68.
- [3] a) D. B. Lao, B. R. Galan, J. C. Linehan, D. J. Heldebrant, *Green Chem.* **2016**, *18*, 4871-4874; b) J. Kothandaraman, R. A. Dagle, V. L. Dagle, S. D. Davidson, E. D. Walter, S. D. Burton, D. W. Hoyt, D. J. Heldebrant, *Catal. Sci. Technol.* **2018**, *8*, 5098-5103; c) S. Xie, W. Zhang, X. Lan, H. Lin, *ChemSusChem* **2020**, *13*, 6141-6159; d) S. Kar, A. Goeppert, G. K. S. Prakash, *Acc. Chem. Res.* **2019**, *52*, 2892-2903; e) N. M. Rezayee, C. A. Huff, M. S. Sanford, *J. Am. Chem. Soc.* **2015**, *137*, 1028-1031; f) J. Kothandaraman, D. J. Heldebrant, *Green Chem.* **2020**, *22*, 828-834; g) M. Scott, B. Blas Molinos, C. Westhues,

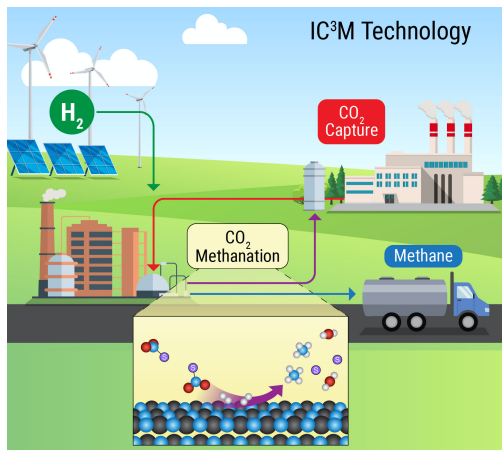
FULL PAPER

- G. Francio, W. Leitner, *ChemSusChem* **2017**, *10*, 1085-1093; h) J. Kothandaraman, A. Goeppert, M. Czaun, G. A. Olah, G. K. Surya Prakash, *Green Chem.* **2016**, *18*, 5831-5838; i) J. Kothandaraman, J. Zhang, V.-A. Glezakou, M. T. Mock, D. J. Heldebrant, *J. CO₂ Util.* **2019**, *32*, 196-201; j) J. W. Maina, J. M. Pringle, J. M. Razal, S. Nunes, L. Vega, F. Gallucci, L. F. Dumee, *ChemSusChem* **2021**, *14*, 1805-1820; k) J. B. Jakobsen, M. H. Ronne, K. Daasbjerg, T. Skrydstrup, *Angew. Chem. Int. Ed.* **2021**, *60*, 9174-9179; l) J. Bi, P. Hou, F. W. Liu, P. Kang, *ChemSusChem* **2019**, *12*, 2195-2201; m) M. Yadav, J. C. Linehan, A. J. Karkamkar, E. van der Eide, D. J. Heldebrant, *Inorg Chem.* **2014**, *53*, 9849-9854; n) R. Sen, C. J. Koch, A. Goeppert, G. K. S. Prakash, *ChemSusChem* **2020**, *13*, 6318-6322; o) E. A. K. Wilson, S. C. Eady, T. Silbaugh, L. T. Thompson, M. A. Barteau, *J. Catal.* **2021**; p) S. Ni, J. Zhu, R. Roy, C.-J. Li, R. B. Lennox, *Green Chem.* **2021**; q) M. Lu, J. Zhang, Y. Yao, J. Sun, Y. Wang, H. Lin, *Green Chem.* **2018**, *20*, 4292-4298; r) J. R. Khushnutdinova, J. A. Garg, D. Milstein, *ACS Catal.* **2015**, *5*, 2416-2422; s) N. D. McNamara, J. C. Hicks, *ChemSusChem* **2014**, *7*, 1114-1124; t) C. Reller, M. Poge, A. Lissner, F. O. Mertens, *Environ. Sci. Technol.* **2014**, *48*, 14799-14804; u) S. Overa, T. G. Feric, A.-H. A. Park, F. Jiao, *Joule* **2021**, *5*, 8-13.
- [4] a) M. Scott, C. G. Westhues, T. Kaiser, J. C. Baums, A. Jupke, G. Francio, W. Leitner, *Green Chem.* **2019**, *21*, 6307-6317; b) J. Kothandaraman, D. J. Heldebrant, *RSC Adv.* **2021**, *10*, 42557 - 42563; c) A. Sternberg, C. M. Jens, A. Bardow, *Green Chem.* **2017**, *19*, 2244-2259; d) J. Klankermayer, W. Leitner, *Science* **2015**, *350*, 629-630; e) Q. Liu, L. Wu, R. Jackstell, M. Beller, *Nat. Commun.* **2015**, *6*, 5933; f) T. Sakakura, J. C. Choi, H. Yasuda, *Chem. Rev.* **2007**, *107*, 2365-2387; g) G. A. Olah, A. Goeppert, G. K. Prakash, *J. Org. Chem.* **2009**, *74*, 487-498; h) J. Klankermayer, S. Wesselbaum, K. Beydoun, W. Leitner, *Angew. Chem. Int. Ed.* **2016**, *55*, 7296-7343; i) C. Song, *Catal. Today* **2006**, *115*, 2-32; j) G. A. Olah, G. K. Prakash, A. Goeppert, *J. Am. Chem. Soc.* **2011**, *133*, 12881-12898; k) S. van Bavel, S. Verma, E. Negro, M. Bracht, *ACS Energy Lett.* **2020**, *5*, 2597-2601; l) Z. Zhang, T. Wang, M. J. Blunt, E. J. Anthony, A.-H. A. Park, R. W. Hughes, P. A. Webley, J. Yan, *Appl. Energy* **2020**, *278*.
- [5] a) R. F. Zheng, D. Barpaga, P. M. Mathias, D. Malhotra, P. K. Koech, Y. Jiang, M. Bhakta, M. Lail, A. V. Rayer, G. A. Whyatt, C. J. Freeman, A. J. Zwoster, K. K. Weitz, D. J. Heldebrant, *Energy Environ. Sci.* **2020**, *13*, 4106-4113; b) Y. Jiang, P. M. Mathias, C. J. Freeman, J. A. Swisher, R. F. Zheng, G. A. Whyatt, D. J. Heldebrant, *Int. J. Greenh. Gas Control.* **2021**, *106*.
- [6] G. Lee, Y. G. C. Li, J. Y. Kim, T. Peng, D. H. Nam, A. S. Rasouli, F. W. Li, M. C. Luo, A. H. Ip, Y. C. Joo, E. H. Sargent, *Nat. Energy* **2021**, *6*, 46-53.
- [7] Natural gas specs sheet, North American Energy Standards Board, <http://www.naesb.org>, last access on 6/30/2021.
- [8] I. S. Omodolor, H. O. Otor, J. A. Andonegui, B. J. Allen, A. C. Alba-Rubio, *Ind. Eng. Chem. Res.* **2020**, *59*, 17612-17631.
- [9] a) M. Younas, L. Loong Kong, M. J. K. Bashir, H. Nadeem, A. Shehzad, S. Sethupathi, *Energy Fuels* **2016**, *30*, 8815-8831; b) W. H. Li, H. Z. Wang, X. Jiang, J. Zhu, Z. M. Liu, X. W. Guo, C. S. Song, *RSC Adv.* **2018**, *8*, 7651-7669.
- [10] a) C. Italiano, J. Llorca, L. Pino, M. Ferraro, V. Antonucci, A. Vita, *Appl. Catal. B: Environ* **2020**, *264*; b) K. Jalama, *Catal. Rev.* **2017**, *59*, 95-164.
- [11] M. H. Wang, A. Ledoux, L. Estel, *J. Chem. Eng. Data* **2013**, *58* (5), 1117-1121.
- [12] a) G. Garbarino, D. Bellotti, E. Finocchio, L. Magistri, G. Busca, *Catal. Today* **2016**, *277*, 21-28; b) B. Miao, S. S. K. Ma, X. Wang, H. Su, S. H. Chan, *Catal. Sci. Technol.* **2016**, *6*, 4048-4058. A possible reaction mechanism for the formation of alcohol and higher hydrocarbons can be found from the following references: c) G. Prieto, *ChemSusChem* **2017**, *10*, 1056-1070; d) R.-P. Ye, J. Ding, W. Gong, M. D. Argyle, Q. Zhong, Y. Wang, C. K. Russell, Z. Xu, A. G. Russell, Q. Li, M. Fan, Y.-G. Yao, *Nat. Commun.* **2019**, *10*, 5698.
- [13] NETL, Cost and Performance Baseline for Fossil Energy Plants, Volume 1a: Bituminous Coal (PC) and Natural Gas to Electricity, Revision 3, DOE/NETL-2015/1723, July **2015**.
- [14] B. Ungerer, C. Weingaertner, H.-P. Dornik, Method of treatment of amine waste water and a system for accomplishing the same, U.S. Patent 9,028,654 B2, filed Feb. 29, **2012** and issued May 12, **2015**.
- [15] P. Marchetti, M. F. Jimenez Solomon, G. Szelely, A. G. Linvingston, *Chem. Rev.* **2014**, *114*, 10735-10806.
- [16] W. L. Becker, M. Penev, R. J. Braun, *J. Energy Resour. Technol.* **2019**, *141*, 021901-021911.
- [17] J. Gao, Y. Wang, Y. Ping, D. Hu, G. Xu, F. Gu, F. Su, *RSC Adv.* **2012**, *2*, 2358-2368.
- [18] IHS Global Inc., Process Economics Program (PEP) Yearbooks, 2014.
- [19] D. C. Cantu, D. Malhotra, M. T. Nguyen, P. K. Koech, D. Zhang, V. A. Glezakou, R. Rousseau, J. Page, R. Zheng, R. J. Perry, D. J. Heldebrant, *ChemSusChem* **2020**, *13*, 3429-3438.
- [20] E. D. Walter, L. Qi, A. Chamas, H. S. Mehta, J. A. Sears, S. L. Scott, D. W. Hoyt, *J. Phys. Chem. C* **2018**, *122*, 8209-8215.

FULL PAPER

Entry for the Table of Contents

Insert graphic for Table of Contents here. ((Please ensure your graphic is in **one** of following formats))



In the presence of a heterogenous Ru catalyst, >90% conversion of captured CO₂ to hydrocarbons, mostly methane, is achieved under relatively mild reaction conditions using a water-lean post-combustion capture solvent. Based on the technoeconomic analyses performed, the proposed integrated process can potentially reduce the total capital investment and minimum synthetic natural gas (SNG) selling price by 32% and 12%, respectively, compared to the conventional Sabatier process.

The Table of Contents text should give readers a short preview of the main theme of the research and results included in the paper to attract their attention into reading the paper in full. The Table of Contents text **should be different from the abstract** and should be no more than 450 characters including spaces.))

Institute and/or researcher Twitter usernames: ((optional))